Steric Strain versus Hyperconjugative Stabilization in Ethane Congeners

Lingchun Song,[†] Yuchun Lin,[‡] Wei Wu,[†] Qianer Zhang,[†] and Yirong Mo*[,†,‡]

Department of Chemistry, State Key Laboratory of Physical Chemistry of Solid Surfaces, Center for Theoretical Chemistry, Xiamen University, Xiamen, Fujian 361005, P. R. China, and Department of Chemistry, Western Michigan University, Kalamazoo, Michigan 49008

Received: November 19, 2004; In Final Form: January 5, 2005

Rotation barriers in the group IVB ethane congeners H_3X-YH_3 (X, Y = C, Si, Ge, Sn, Pb) have been systematically studied and deciphered using the ab initio valence bond theory in terms of the steric strain and hyperconjugation effect. Our results show that in all cases the rotation barriers are dominated by the steric repulsion whereas the hyperconjugative interaction between the X−H bond orbitals and the vicinal Y−H antibond orbitals (and vice versa) plays a secondary role, although indeed the hyperconjugation effect favors staggered structures. By the independent estimations of the hyperconjugative and steric interactions in the process of rotations, we found that the structural effect which mainly refers to the central X−Y bond relaxation makes a small contribution to the rotational barriers. Therefore, we conclude that both the rigid and fully relaxed rotations in the group IVB ethane congeners H_3X-YH_3 observe the same mechanism which is governed by the conventional steric repulsion.

Introduction

A molecular conformation is usually determined by the interactions among bonds which form the molecule. Apart from the steric repulsion (mostly Pauli exchange interaction) among the bonds, stabilizing forces among π bonds (conjugation) or π and σ bonds (hyperconjugation) play important roles in the determination of the most favorable conformation.[1] Although there have been speculations for the possible hyperconjugative interaction among σ bonds,[2] there are few straightforward ways to distinguish the usually competing steric and hyperconjugative effects, and theoretical analyses heavily depend on how the steric and electronic interactions are computationally formulated as various approximations must be introduced in the formulations.[3−5] This is exactly the case for ethane, which has been conventionally and intuitively believed that the staggered structure is favored over the eclipsed structure due to the repulsive exchange interactions between the electrons in the two methyl groups,[6] and this simple repulsion model was confirmed by earlier ab initio bond orbital calculations.[3,7] Later, Weinhold and coworkers showed that hyperconjugative interaction between the σ_{CH} occupied orbitals in one methyl group and the σ_{CH}* antibonding orbitals in the other methyl group stabilizes the staggered conformer on the basis of a bond orbital analysis at both the semiempirical and ab initio levels.[8−10] However, it is Pophristic and Goodman's recent work, which is also based on Weinhold's natural bond orbital (NBO) method, that refuels the debate over the nature of the ethane rotation barrier.[11−13] Pophristic and Goodman surprisingly concluded that the Pauli exchange energy actually stabilizes the eclipsed conformer of ethane relative to the gauche conformer.[13] In other words, the eclipsed structure would be preferred if the hyperconjugative interaction was quenched. Another puzzling finding by these authors is that a slight variation (0.014 Å) of the central C−C bond is essential for the hyperconjugation theory, implying that the rigid rotation and fully relaxed rotation have different mechanisms for the barriers, although their numerical values are very close. Furthermore, Goodman and co-workers found that the mechanism governing the ethane rotation barrier does not apply to ethane congeners such as disilane and digermane.[14,15]

SCHEME 1

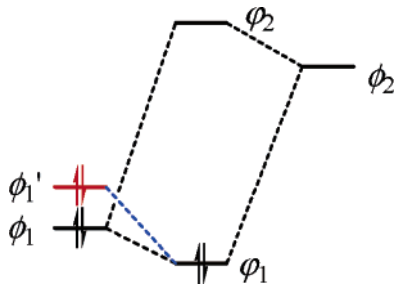

The justification of either the steric repulsion model or the hyperconjugative attraction model requires a deep investigation into the theoretical methods used in the calculations. In the molecular orbital (MO) theory, the hyperconjugative stabilization comes from the interaction between an occupied localized orbital (e.g., bond orbital σ_{CH} in ethane) and a virtual localized orbital (e.g., σ_{CH}*),[16] and subsequently, the hyperconjugation energy is defined as the energy difference between the occupied localized orbital ϕ_1 and the occupied delocalized orbital φ_1 as illustrated in Scheme 1. However, in the MO theoretical calculations, only delocalized orbitals $\{\varphi\}$ can be obtained self-consistently. Assumptions have to be adopted to derive localized orbitals $\{\phi\}$. If the latter are not optimal, their orbital energies will be lifted to high levels (e.g., ϕ_1' in Scheme 1) and a severe consequence is the overestimation of the hyperconjugation energy. As one of the post self-consistent-field (SCF) approaches to derive localized MOs,[17] the NBO method is designed to substrate localized bond orbitals from a delocalized wave function in order to construct the localized Lewis structure.[8] It

* To whom correspondence should be addressed. E-mail: yirong.mo@wmich.edu.
† Xiamen University.
‡ Western Michigan University.

10.1021/jp044700s CCC: $30.25
Published on Web 02/16/2005

is of general interest and importance to scrutinize how the electronic relaxation or optimization for the Lewis structure may influence the estimation of the hyperconjugation energy and eventually the interpretation for the origin of the ethane rotation barrier.

The most recent studies by Bickelhaupt and Baerends[18] and us[19] using very different methods consistently demonstrated that the steric hindrance dominates the ethane rotation barrier, although the hyperconjugative interaction does favor the staggered conformation. Bickelhaupt and Baerends built a zeroth-order wave function for ethane with fragmental molecular orbitals of the two methyl groups to directly evaluate the Pauli and electrostatic interactions.[18] They concluded the steric repulsion as the driving force for the barrier in ethane, although the zeroth-order wave function used in their analysis was neither optimized self-consistently nor an eigenfunction of the spin operator.[20] Alternatively, we adopted the ab initio valence bond (VB) method to construct both the localized (Lewis structure) and delocalized wave functions self-consistently and compute the hyperconjugative stabilization explicitly in both the staggered and eclipsed structures.[19] We found that the hyperconjugation effect does favor the staggered structure but accounts for only around one-third of the rotation barrier, most of which comes from the steric hindrance which is independently estimated by freezing all bond orbitals in the process of rotation. Notably, most recent experimental proofs supported the repulsion explanation for the ethane rotation barrier.[21]

In this work, we extended our ab initio VB studies to the all group IVB ethane congeners H_3X-YH_3 (X, Y = C, Si, Ge, Sn, Pb) and elucidated their rotation barriers in terms of the steric strain and hyperconjugation effect. Schleyer and co-workers have extensively examined the structures and rotational barriers in these 15 H_3X-YH_3 hydrides.[22] With the NBO method, they explored the nature of rotational barriers in terms of vicinal $\sigma_{XH} \rightarrow \sigma_{YH}^*$ and $\sigma_{XH} \rightarrow \sigma_{YH}^*$ interactions. On the basis of the modern ab initio VB theory, we found that all barriers in both rigid and fully relaxed rotations are consistently dominated by the steric repulsion, although the hyperconjugative interaction uniformly prefers the staggered structures. Thus, the mechanisms for the rotations around X−Y single bonds in these systems are identical and the concept of steric repulsion holds.

Methodology

Compared with the orbital interaction picture in the MO theory, the VB theory is established on resonance structures, and thus, a molecule is described by a set of resonance structures.[6,23] Theoretically, each resonance structure can be represented by a Heilter−London−Slater−Pauling (HLSP) function, which can be expanded into a linear combination of 2^m Slater determinants (m is the number of covalent bonds in the focused system) or by its equivalent spin-free form such as the bonded tableau used in our approach.[24] The most prominent difference between MO and VB theories is that in VB theory all orbitals are nonorthogonal, whereas molecular orbitals are restrained to be orthogonal in MO theory. In the extreme end (i.e., full CI), however, these two theories are equivalent.

In our approach, the VB wave function for each resonance structure is defined with a spin-free form as[24]

$$\Phi_K = N_K e_{r1}^{[\lambda]} \Omega_K \tag{1}$$

where N_K is a normalization factor, $e_{r1}^{[\lambda]}$ is a standard projection operator of symmetry group for irreducible representation $[\lambda]$ in the orbital space, and Ω_K is simply an orbital product

$$\Omega_K = \varphi_{i_1}(1)\varphi_{j_1}(2)\varphi_{i_2}(3)\varphi_{j_2}(4)\cdots \tag{2}$$

Equation 2 corresponds to a resonance structure with bonds between i_1 and j_1, i_2 and j_2, and so on. An equivalent expression for eq 1 (hereby we assume the total spin quantum number $S = 0$) is

$$\Phi_K = N_K \hat{A}(\phi_{i_1 j_1}\phi_{i_2 j_2}\cdots\phi_{i_m j_m}) \tag{3}$$

where $\hat{A}$ is the antisymmetrizer and $\phi_{i,j}$ is simply a bond function corresponding to the bond between orbitals φ_i and φ_j

$$\phi_{ij} = \hat{A}\{\varphi_i\varphi_j[\alpha(i)\beta(j) - \beta(i)\alpha(j)]\} \tag{4}$$

where the spins of electrons (α and β) are explicitly considered and both φ_i and φ_j are expanded with the basis functions centered on the two bonding atoms and called as bond-distorted orbitals (BDOs).[25] Equation 4 highlights that a bond orbital is not only a singlet spin eigenfunction but also comprised of two Slater determinants. The wave function for the molecule is subsequently expressed as a linear combination of spin-free VB functions

$$\Psi = \sum_K C_K \Phi_K \tag{5}$$

Although the VB concepts are much familiar to chemists and the VB theory was proposed even earlier than the MO theory, the bottleneck in the ab initio VB method lies in the evaluations of the overlap and Hamiltonian matrix elements among VB functions where orbitals are nonorthogonal. In contrast, the orthogonality restraint among MOs makes the MO-based methods extremely efficient. Unfortunately, the popularity of the MO methods has been accompanied with a few misunderstandings for the VB theory as eloquently addressed very recently by Hoffman and co-workers,[26] and the ultimate truth is that the MO and VB theories are supplementary and consistent rather than conflicting and competing. During the past decade, modern ab initio VB methods have been developed with a few practical codes available.[27−30] Applications have distinctively demonstrated the importance of the VB approaches in gaining new insights into molecular structures, properties, and reactivity, which provide understandings to the results obtained from MO computations from different perspectives. In the quest for efficient algorithms in the ab initio VB computations, we introduced a new function called paired-permanent-determinant (PPD), which is an algebrant.[29] The introduction of PPD reduces the CPU and memory requirements and eventually makes the treatment of systems such as ethane and its congeners straightforward. In the present version of our code, XMVB,[30] an algorithm of $2 \times (N - 2)$ expansion is used since 1-e and 2-e electronic integrals can be built as "effective" 2×2 PPDs.

Calculation Details

The MO theory interprets the hyperconjugative interaction in terms of localized orbitals (Scheme 1), whereas in the terminology of VB theory, the hyperconjugation effect in ethane congeners H_3X-YH_3 (X, Y = C, Si, Ge, Sn, Pb) can be mainly described by the following three kinds of resonance structures (Scheme 2). Covalent resonance structure **I** is the most stable one among all, and biradical structures **II** are more stable than ionic structures **III** in the gaseous phase. In total there are 9 biradical structures **II** and 18 singly ionic structures **III**. Consequently, the overall wave function Ψ for H_3X-YH_3 is a superposition of a total of 28 resonance structures and the energy

SCHEME 2

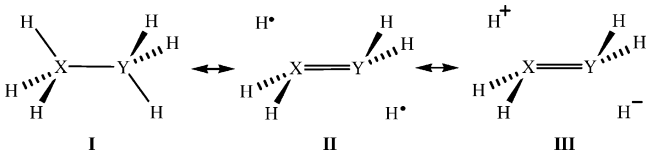

I **II** **III**

difference between Ψ and the most stable resonance structure Φ_I corresponds to the hyperconjugative stabilization. The solution of Ψ thus is a multi-structure self-consistent-field procedure which is comparable to the MCSCF method in the MO theory.

We start from the construction of the covalent structure **I** with a HLSP function

$$\Phi_I = \hat{A}(K_X K_Y \sigma_{XY} \sigma_{XH_1} \sigma_{XH_2} \sigma_{XH_3} \sigma_{YH_4} \sigma_{YH_5} \sigma_{YH_6}) \qquad (6)$$

where K_X and K_Y refer to the core orbitals and lone pairs on atoms X and Y and each bond orbital σ_{ij} is localized on the two bonding atoms i and j only. In principle, wave functions for biradical and ionic resonance structures can be written out similarly, and the simultaneous optimization of the orbitals and configuration coefficients results in the overall wave function Ψ.

However, the most important feature of modern ab initio VB methods is that orbitals are allowed to expand and optimize flexibly.[25,28] The use of overlap-enhanced orbitals (OEOs),[31] which are expanded in the whole molecular space like regular MOs, provides the key to the construction of VB functions of considerable accuracy and compactness. Since normally neutral covalent resonance structures are much more stable than radical and ionic resonance structures, using OEOs and only neutral covalent structures can recover the electron correlations overwhelmingly. For example, for benzene, Cooper et al. have demonstrated that over 93% of electron correlation can be recovered by two Kékule and three Dewar structures.[32] For the current cases of ethane congeners, there are high energy gaps between the stable covalent structure and the rest biradical or ionic structures which have a long separation of unpaired electrons or charges and the unfavorable orientation of the double bond character between two carbons. Thus, we skip the biradical and ionic structures by using delocalized OEOs and define the wave function for H_3X-YH_3 as

$$\Psi = \hat{A}(K_X K_Y \sigma_{XY}' \sigma_{XH_1}' \sigma_{X_1H_2}' \sigma_{XH_3}' \sigma_{YH_4}' \sigma_{YH_5}' \sigma_{YH_6}') \qquad (7)$$

where orbital σ_{ij}' adopts the form of eq 4 using φ_i' and φ_j' that are expanded in the whole basis space of the molecule, rather than the subspace of two bonding atoms as φ_i and φ_j in Φ_I. Once the localized and delocalized wave functions are defined as in eqs 6 and 7, the hyperconjugation stabilization energy in ethane E_{hc} can be estimated as the energy difference between them

$$E_{hc} = E(\Psi) - E(\Phi_I) = \langle \Psi | \hat{H} | \Psi \rangle - \langle \Phi_I | \hat{H} | \Phi_I \rangle \qquad (8)$$

where $\hat{H}$ is the Hamiltonian operator. It should be pointed out that both Ψ and Φ_I can be expanded into $2^7 = 128$ Slater determinants, and in our code, all orbitals $\{\varphi_i\}$ and $\{\varphi_i'\}$ are optimized self-consistently and in total the VB part contains 14 electrons.

It has been well recognized that the geometries and rotational barriers in ethane and its congeners are rather insensitive to the basis sets and theoretical levels used.[12,22,33] Thus, we adopt the geometries optimized at the HF level with the basis sets of 6-31G(d) for C and Si and Los Alamos effective core potential and matching basis set, LANL2DZ[34] augmented with d-polarization functions[35] (henceforth LANL2DZd) for Ge, Sn, and Pb for further VB calculations. In the case of ethane, we have shown that the enlargement of the basis set from 6-31G(d) to 6-311G(d,p) does not alter the results and conclusions at all. In this work, we similarly examine the basis set dependence for disilane. Geometry optimizations and HF energy calculations as well as the primitive integrals that are required for the subsequent VB calculations were carried out using Gaussian98,[36] while VB calculations were performed with our XMVB program.[30]

Results and Discussion

Hyperconjugative Interaction in Disilane. Ab initio VB calculation results with the 6-31G(d) and 6-311G(d,p) basis sets for the localized and delocalized structures of disilane were compiled in Table 1, where ΔE_{hc} denotes the hyperconjugation energy (E_{hc}) difference between the eclipsed and staggered structures. It is particularly interesting to note that even the VB energies for the localized (Lewis) structures ($E(\Phi_I)$ in Table 1) are considerably lower than the respective HF energies $E(\Psi)$, because electron correlation is taken into account in the construction of VB functions by keeping the pairing electrons apart. For comparison, Table 1 also listed the hyperconjugation energies computed with the NBO method. Within the NBO method, hyperconjugation energies can be computed by deleting either off-diagonal elements (NBO1) or antibond orbitals (NBO2). An increase of the VB hyperconjugation energies is observed with the enlargement of the basis set from 6-31G(d) to 6-311G(d,p), whereas the NBO energies are a little more stable than the VB data. This phenomenon has two origins. One is the artifact of basis sets, but this concern exists in all methods. The other is that in our calculations we only consider 14 electrons in the VB part, whereas unlike carbon, each Si atom has additional six 2p electrons which may get slightly involved in the hyperconjugative interaction between two silyl moiety groups in disilane. A further improvement is to localize 2p electrons in the covalent resonance structure. This can be achieved by our newly developed block-localized wave function (BLW) method, which does show little basis set dependency in the calculations of delocalization energies.[37,38]

Even with the basis set of 6-31G(d), however, we still found significant hyperconjugative interactions in both the staggered and eclipsed structures of disilane, which are even comparable to the $\sigma-\pi$ hyperconjugation in propane, as both experimental and theoretical studies suggested a stabilizing effect of around 3−5 kcal/mol.[37,39] Part of the hyperconjugation energies listed in Table 1 actually should be ascribed to the geminal bond−antibond interactions between silyl groups and the Si−Si bond and antibond, as pointed out by Reed and Weinhold.[10] This also explains why the second set of NBO data is much larger than the first set of data (Table 1). These geminal interactions are invariable with respect to internal rotations due to symmetry, and thus, only the difference between the staggered and eclipsed structures is the focal point in our current investigation of the nature of the rotational barriers, as verified by the BLW calculations in the ethane case.[19] Indeed, both the VB and NBO calculations show negligible basis set dependency for the hyperconjugation energy differences. Whereas both methods confirmed that the vicinal $\sigma_{SiH} \rightarrow \sigma_{SiH}^*$ hyperconjugative interaction favors the staggered structure of disilane, the VB calculations show that the hyperconjugation energy difference is only about 0.25−0.28 kcal/mol, compared with the rotational

TABLE 1: Hyperconjugation Energies in Disilane Computed with the ab Initio VB Method and NBO Method at the HF/6-31G(d) Optimal Geometries

	6-31G(d)[a]		6-311G(d,p)[b]	
energy	staggered	eclipsed	staggered	eclipsed
$E(\Phi_I)$ (a.u.)	−581.39003	−581.38914	−581.43561	−581.43468
$E(\Psi)$ (a.u.)	−581.39567	−581.39439	−581.44510	−581.44372
E_{hc} (kcal/mol)	−3.54	−3.29	−5.95	−5.67
ΔE_{hc} (kcal/mol)	0.0	0.25	0.0	0.28
E_{hc} (NBO1) (kcal/mol)[c]	−7.32	−6.12	−5.11	−4.22
ΔE_{hc} (NBO1) (kcal/mol)	0.0	1.20	0.0	0.89
E_{hc} (NBO2) (kcal/mol)[d]	−30.80	−29.68	−31.65	−30.63
ΔE_{hc} (NBO2) (kcal/mol)	0.0	1.12	0.0	1.02

[a] HF energies for the staggered and eclipsed conformers are −581.30509 and −581.30358 au, respectively, corresponding to a barrier of 0.95 kcal/mol. [b] HF energies for the staggered and eclipsed conformers are −581.35592 and −581.35436 au, respectively, corresponding to a barrier of 0.98 kcal/mol. [c] The NBO delocalization energies are computed based on the deletion of off-diagonal elements between Si−H bond orbitals in one moiety and Si−H antibond orbitals in the other moiety. Totally 18 elements are deleted. [d] The NBO delocalization energies are computed based on the deletion of six Si−H antibond orbitals.

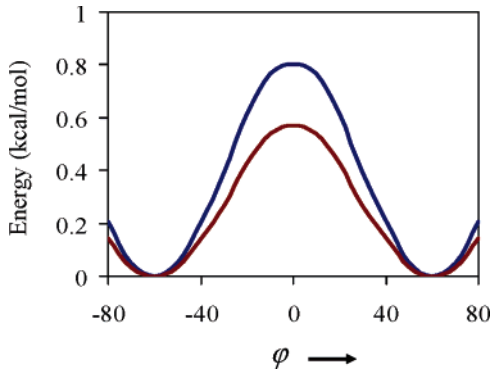

Figure 1. Comparison of energy profiles for the disilane rotation where the hyperconjugation effect is considered (blue line) or screened out (brown line).

barrier 0.80−0.87 kcal/mol at the same VB level. Although the experimental value for the disilane rotation barrier is 1.26 kcal/mol,[40] theoretical calculations at various levels give a range of 0.82−1.09 kcal/mol.[14,22,41] The ab initio VB results suggest that the attractive hyperconjugation effect is far from being able to account for the total rotational barrier. In contrast, the NBO calculations resulted in a large hyperconjugation energy difference of 1.08−1.20 kcal/mol, compared with the barrier 0.95−0.98 kcal/mol at the HF level. The NBO data implies that if there were no hyperconjugative interaction the silyl groups can rotate almost freely in disilane. The difference between the ab initio VB and NBO results reinstates the importance of relaxing the wave function of the Lewis structure, which is self-consistently optimized in the VB calculations.

Depicted in Figure 1 are the torsional energy profiles determined with (blue curve, Ψ in eq 7) and without (brown curve, Φ_I in eq 6) the contribution of hyperconjugative interactions in disilane from VBSCF/6-31G(d) calculations. The energy profile that has the hyperconjugation effect screened out essentially corresponds to effects due to the Pauli exchange and electrostatic repulsion interactions or steric effects. Our results demonstrate that when hyperconjugative interactions in disilane are excluded, the staggered structure is still favored over the eclipsed conformation by 0.55−0.59 kcal/mol.

Steric Strain in Disilane. Although it is generally assumed that the rotational barrier comes from the attractive electronic effect (hyperconjugation) and the repulsive steric effect and the latter can be conveniently determined by subtracting the hyperconjugation energy from the overall rotational barrier, it is desirable to evaluate the steric energy independently. In the analysis on ethane, we proposed a solution to probe the energetic

TABLE 2: Energy Variation by Freezing the Bond Orbitals during the Rotation in Disilane (kcal/mol)

	staggered → eclipsed[a]	eclipsed → staggered[b]
basis set	ΔE_{steric}	ΔE_{steric}
6-31G(d)	0.57	−0.56
6-311G(d,p)	0.59	−0.57

[a] Starting from the optimal VB function for the staggered conformer. [b] Starting from the optimal VB function for the eclipsed conformer.

variation by freezing the bond orbitals $\{\phi_{ij}\}$ during the rotation where the hyperconjugation effect is deactivated. The procedure is as follows. First, we obtain the optimal VB function Φ_I for the covalent structure at the initial geometry (either staggered or eclipsed) self-consistently. Second, we rotate one silyl group by 60° to the optimal eclipsed (or staggered) structure and recompute the energy by fixing all bond orbitals without any SCF calculation. In this step, a Jacobi 2 × 2 matrix transformation is applied to the *p* and *d* orbitals of the rotated silyl group. Finally, we estimate the energy change along the rotation and ascribe this energy change to the steric effect, as in this procedure all orbitals are frozen and no electronic relaxation occurs. In the above procedure of rotation, disilane is structurally relaxed but electronically frozen, and in general the computed steric energy is comprised of Pauli exchange repulsion and electrostatic interaction (including the dispersion energy). A small amount of geometric effect (mostly the variation of the central Si−Si bond length) has also been included into this steric energy term and will be discussed further in the next section. With this procedure, we computed the steric energy change in the process of rotation from the staggered to the eclipsed conformation when all orbitals are frozen but structural parameters are flexed and vice versa with the 6-31G(d) and 6-311G(d,p) basis sets. Results are summarized in Table 2. In either direction, the results are very similar and independent of basis sets used in the calculations, and the steric effect contributes about 0.6 kcal/mol to the disilane rotation barrier, which is twice as large as the hyperconjugation stabilization. The slight difference (0.01−0.02 kcal/mol) between the rigid rotation processes using bond orbitals optimized either at the staggered or eclipsed conformation is due to the small difference between the electronic structures in the two conformers, namely the electronic relaxation in the rotation. These findings are identical to those in the ethane case, indicating that both systems have the very same rotation mechanism.

Structural Effect in Disilane. Researchers in favor of the attractive explanation for rotation heights around single bonds also found that the interpretation of barriers is influenced by

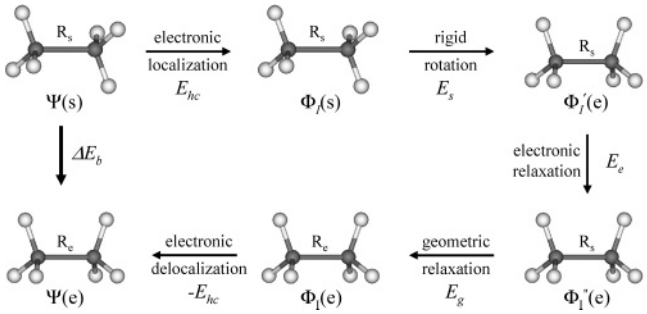

Figure 2. Decomposition scheme to explore the geometric impact on the rotational barrier.

the slight change of the central bond lengths. In other words, rigid rotations and fully relaxed rotations, albeit they have very close barriers, may have different rotation mechanisms.[5,9,13,14] At the HF/6-31G(d) level, the optimal Si−Si bond distance in the staggered structure (2.352 Å) is 0.010 Å shorter than that in the eclipsed structure (2.362 Å). Although in the pretext we have independently examined both the hyperconjugation and steric effects and their total energy contributions are very close to the overall barrier, it is illuminating to discern the electronic and geometric relaxations, particularly in the central Si−Si bond, in the process of rotation. As we mentioned in the above, the geometric effect has been contained in the steric energies in Table 2. Here we propose to probe the structural effect on the rotational barrier in the following five successive steps as shown in Figure 2: (1) at the optimal geometry of the staggered structure, deactivate the hyperconjugation effect. The energy variation in this step is the reverse of the hyperconjugation energy defined by eq 8 in the staggered structure ($-E_{hc} = 3.54$ or 5.95 kcal/mol with 6-31G(d) or 6-311G(d,p)); (2) freeze all orbitals and structural parameters except the dihedral angle between the two silyl groups and rotate one group by 60° to the eclipsed structure. Energy changes in this step come from the steric repulsion in the rigid rotation ($E_s = 0.69-0.72$ kcal/mol); (3) relax the electrons in the covalent resonance structure. The re-optimization of the bond orbitals inherited from the staggered structure will negligibly stabilize the covalent structure ($E_e = -0.002$ kcal/mol with both basis sets); (4) relax the geometry to the optimal eclipsed structure for the covalent resonance structure. The geometric change is dominated by the lengthening of the Si−Si bond by 0.010 Å and the accompanied energy reduction results from the structural effect ($E_g = -0.13$ kcal/mol with 6-31G(d) and −0.14 kcal/mol with 6-311G(d,p)); (5) allow the electrons to delocalize among the two silyl groups which is the hyperconjugation effect in the eclipsed structure ($E_{hc} = -3.29$ or −5.67 kcal/mol with 6-31G(d) or 6-311G-(d,p)).

On the basis of the above energy decomposition, we found that the electronic relaxation (E_e) causes unnoticeable energy changes in the rotation, whereas the geometric relaxation (E_g) which lengthens the central Si−Si bond from the staggered conformer to the eclipsed conformer slightly stabilizes the system. These results prompt us to conclude that the slight central bond perturbation in the rotation makes very limited energy contribution to the rotation barrier in disilane. This is apparently consistent with the fact that the rigid rotational barrier is only slightly higher (0.03 kcal/mol[14]) than the relaxed rotation barrier, and therefore, both have the same mechanism which is dominated by the steric effect.

General Trends in all Ethane Congeners. With the same approaches described in the above, we continued our analyses to the whole set of 15 group IVB ethane congeners H_3X-YH_3 (X, Y = C, Si, Ge, Sn, Pb). Computation results are collected in Tables 3 and 4. In accord with our detailed analyses on ethane and disilane, we found that in all systems the hyperconjugation effect stabilizes the staggered structures more than the eclipsed structures, but the hyperconjugation energy changes between the staggered and eclipsed structures are small compared with the overall rotational barriers, which are dominated by the steric repulsion in all ethane congeners. Schleyer et al. have already found that the barriers decrease with the increasing of the X−Y bond distances.[22] Our decomposition of the rotation barriers in terms of steric and hyperconjugative interactions reveals that the percentage contribution of the steric repulsion to the rotation barriers increases with the increasing of the X−Y bond distances, whereas the percentage contribution of the hyperconjugative interaction to the rotation barriers decreases (Figure 3). From the MO theory perspective, both steric and hyperconjugative interactions are related with the overlap magnitudes of the adjacent XH_3 and YH_3 moieties which depend on the

TABLE 3: Hyperconjugative Stabilization in Staggered and Eclipsed Structures and the Steric and Hyperconjugative Contributions to the Rotation Barriers in Ethane Congeners H_3X-YH_3(X,Y = C, Si, Ge, Sn, Pb) with the Basis Sets of 6-31G(d) for C and Si and LANL2DZ(d) for Ge, Sn, and Pb (kcal/mol)

X−Y	E_{hc} (s)	E_{hc} (e)	ΔE_{hyp}[a]	ΔE_{st}[b]	ΔE_b (VB)	ΔE_b (HF)	ΔE_b (MP2)[c]	ΔE_b (expt)[d]
C−C	−11.08	−10.18	0.90	1.80	2.71	2.99	3.14	2.88
C−Si	−6.00	−5.59	0.41	0.86	1.27	1.40	1.54	1.69
C−Ge	−8.32	−7.97	0.35	0.75	1.10	1.21	1.25	1.24
C−Sn	−6.21	−6.08	0.13	0.44	0.57	0.61	0.70	0.65
C−Pb	−6.21	−6.14	0.08	0.32	0.39	0.42	0.51	
Si−Si	−3.54	−3.29	0.24	0.57	0.80	0.95	1.07	1.26
Si−Ge	−5.08	−4.93	0.15	0.58	0.73	0.84	0.85	
Si−Sn	−4.06	−4.00	0.06	0.46	0.52	0.58	0.55	
Si−Pb	−4.28	−4.23	0.04	0.36	0.40	0.47	0.43	
Ge−Ge	−7.79	−7.67	0.12	0.49	0.61	0.71	0.72	
Ge−Sn	−6.15	−6.08	0.07	0.40	0.46	0.52	0.51	
Ge−Pb	−6.38	−6.34	0.04	0.32	0.36	0.42	0.41	
Sn−Sn	−5.13	−5.11	0.02	0.34	0.36	0.43	0.42	
Sn−Pb	−5.37	−5.35	0.02	0.28	0.30	0.36	0.35	
Pb−Pb	−5.55	−5.54	0.01	0.23	0.24	0.30	0.29	

[a] ΔE_{hyp} is defined as the hyperconjugation energy difference between the eclipsed and staggered structures, i.e., $\Delta E_{hyp} = E_{hc}(e) - E_{hc}(s)$. [b] $\Delta E_{st} = \Delta E_b(VB) - \Delta E_{hyp}$. [c] MP2 rotation barriers are computed at the HF optimal geometries. [d] References 42 and 40.

TABLE 4: Estimation of the Steric Effect by Freezing the Bond Orbitals during the Rotation in Ethane Congeners H_3X-YH_3(X,Y=C, Si, Ge, Sn, Pb) with the Basis Sets of 6-31G(d) for C and Si and LANL2DZp for Ge, Sn and Pb (kcal/mol)

X−Y	staggered → eclipsed[a]	eclipsed → staggered[b]
C−C	1.85	−1.76
C−Si	0.88	−0.84
C−Ge	0.77	−0.73
C−Sn	0.45	−0.43
C−Pb	0.33	−0.31
Si−Si	0.57	−0.56
Si−Ge	0.59	−0.57
Si−Sn	0.46	−0.45
Si−Pb	0.36	−0.35
Ge−Ge	0.50	−0.48
Ge−Sn	0.40	−0.39
Ge−Pb	0.32	−0.31
Sn−Sn	0.34	−0.34
Sn−Pb	0.29	−0.28
Pb−Pb	0.23	−0.23

[a] Starting from the optimal VB function for the staggered conformer. [b] Starting from the optimal VB function for the eclipsed conformer.

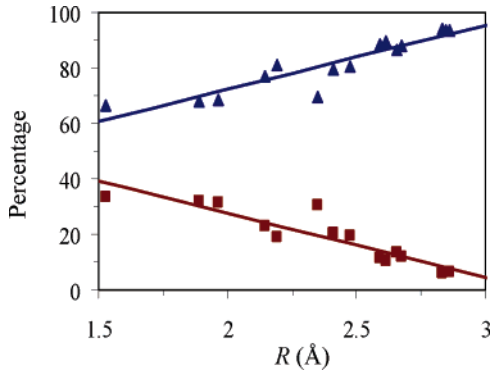

Figure 3. Correlations between the relative contributions of steric effect (in blue) and hyperconjugation effect (in brown) to the rotation barriers versus the central X−Y bond distances in all ethane congeners.

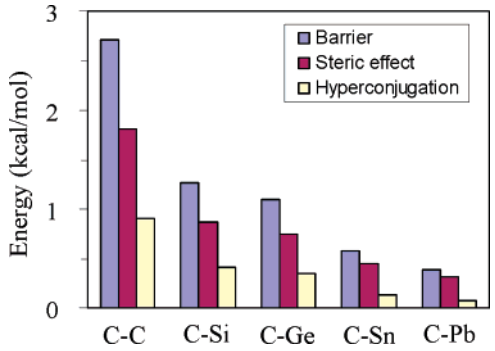

Figure 4. Variations of the rotation barriers and their steric and hyperconjugation components in CH_3-YH_3 (Y = C, Si, Ge, Sn, Pb)

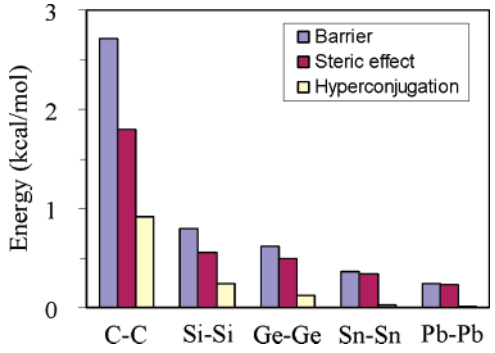

Figure 5. Variations of the rotation barriers and their steric and hyperconjugation components in X_2H_6 (X = C, Si, Ge, Sn, Pb)

X−Y distances, but it seems from Figure 3 that the hyperconjugation effect decays faster than the steric effect with the stretching of the central X−Y bond.

Straight correlations can be derived when we focus on systems with the same XH_3 group and variable YH_3 groups. Figure 4 shows the overall rotation barriers together with the corresponding steric and hyperconjugation energy changes in CH_3-YH_3 (Y = C, Si, Ge, Sn, Pb) systems. With the decreasing of the electronegativity in the order of C > Si > Ge > Sn > Pb and the increasing of atomic radius as well as the donor ability of YH bonds in the reverse order, the rotation barriers decrease from up to low in the IVB main group and so do their energy components of the steric and hyperconjugation effects. In all systems, the steric repulsion makes the dominant contribution to the rotation barriers, whereas the hyperconjugation plays a secondary role and its magnitude is less than half of steric effect. Similar trends can be found in other series of systems.

Figure 5 shows the changes of the rotation barriers, steric and hyperconjugation energies in the five X_2H_6 (X = C, Si, Ge, Sn, Pb) systems. Compared with Figure 4, all energy terms decrease at higher rates. However, the general rules stand firmly.

Conclusion

Exploration of the nature of the rotational barriers in the whole set of ethane congeners H_3X-YH_3 (X, Y = C, Si, Ge, Sn, Pb) with the modern ab initio VB theory reveals that the hyperconjugative interactions between vicinal XH and YH bonds does favor the staggered structures in all cases, which is in qualitative agreement with the hyperconjugation model.[2,9−15] However, the magnitude of the hyperconjugation contribution to the barriers is much lower than the overall rotation barriers. The exclusion of all electronic effects by freezing all orbitals in the rotations demonstrated that the majority of the rotation barrier in H_3X-YH_3 comes from the steric repulsion. Stepwise analyses on disilane further show that the central Si−Si bond stretching stabilizes the system by 0.13−0.14 kcal/mol which is a small fraction of the rotation barrier. Based on the modern ab initio VB calculations, we summarize that both the rigid and fully relaxed rotations in ethane congeners follow the same mechanism that the steric repulsion is the primary cause for the barrier, while the hyperconjugation effect plays a secondary role.

Acknowledgment. The research at XMU is supported by the Natural Science Foundation of China (Grant Nos. 20225311, 20373052, and 20021002). Support from the Western Michigan University is gratefully acknowledged (Y.M.).

References and Notes

(1) (a) Mo, Y.; Song, L.; Wu, W.; Cao, Z.; Zhang, Q. *J. Theor. Comput. Chem.* **2002**, *1*, 137. (b) Mo, Y. *Curr. Org. Chem.* **2005**, to be published.

(2) (a) Mulliken, R. S. *J. Chem. Phys.* **1939**, *7*, 339. (b) Lowe, J. *J. Am. Chem. Soc.* **1970**, *92*, 3799. (c) England, W.; Gordon, M. S. *J. Am. Chem. Soc.* **1971**, *93*, 4649. (d) Epiotis, N. D.; Cherry, W. R.; Shaik, S.; Yates, R. L.; Bernardi, F. *Topics in Current Chemistry: Structural Theory of Organic Chemistry*; Springer-Verlag: Berlin, 1977; Vol. 70.

(3) Sovers, O. J.; Kern, C. W.; Pitzer, R. M.; Karplus, M. *J. Chem. Phys.* **1968**, *49*, 2592.

(4) (a) Allen, L. C. *Chem. Phys. Lett.* **1968**, *2*, 597. (b) Payne, P. W.; Allen, L. C. In *Mordern Theoretical Chemistry*; Schaefer, H. F., III, Ed.; Plenum Press: New York, 1977; Vol. 4, p 29. (c) Csizmadia, I. G. *Theory and Practice of MO Calculations on Organic Molecules*; Elsevier: New York, 1976. (d) Knight, E. T.; Allen, L. C. *J. Am. Chem. Soc* **1995**, *117*, 4401. (e) Sadlej-Sosnowska, N. *J. Phys. Chem. A* **2003**, *107*, 8671.

(5) Bader, R. F. W.; Cheeseman, J. R.; Laidig, K. E.; Wiberg, K. B.; Breneman, C. *J. Am. Chem. Soc.* **1990**, *112*, 6530.

(6) Pauling, L. C. *The Nature of the Chemical Bond*; 3rd ed.; Cornell University Press: Ithaca, NY, 1960.

(7) Hoyland, J. R. *J. Am. Chem. Soc.* **1968**, *90*, 2227.

(8) (a) Brunck, T. K.; Weinhold, F. *J. Am. Chem. Soc.* **1979**, *101*, 1700. (b) Reed, A. E.; Curtiss, L. A.; Weinhold, F. *Chem. Rev.* **1988**, *88*, 899.

(9) Corcoran, C. T.; Weinhold, F. *J. Chem. Phys.* **1980**, *72*, 2866.

(10) Reed, A. E.; Weinhold, F. *Isr. J. Chem.* **1991**, *31*, 277.

(11) (a) Goodman, L.; Gu, H. *J. Chem. Phys.* **1998**, *109*, 72. (b) Goodman, L.; Pophristic, V.; Weinhold, F. *Acc. Chem. Res.* **1999**, *32*, 983.

(12) Goodman, L.; Gu, H.; Pophristic, V. *J. Chem. Phys.* **1999**, *110*, 4268.

(13) Pophristic, V.; Goodman, L. *Nature* **2001**, *411*, 565.

(14) Pophristic, V.; Goodman, L.; Wu, C. T. *J. Phys. Chem. A* **2001**, *105*, 7454.

(15) Goodman, L.; Pophristic, V.; Wang, W. *Int. J. Quantum Chem.* **2002**, *90*, 657.

(16) (a) Wheland, G. W. *J. Chem. Phys.* **1934**, *2*, 474. (b) Cramer, C. J. In *Encyclopedia of Computational Chemistry*; Schelyer, P. v. R., Ed.; John Wiley & Sons: Berlin, 1998; p 1294.

(17) (a) Foster, J. M.; Boys, S. F. *Rev. Mod. Phys.* **1960**, *32*, 300. (b) Edmiston, C.; Ruedenberg, K. *Rev. Mod. Phys.* **1963**, *35*, 457. (c) Edmiston, C. *THEOCHEM* **1988**, *46*, 331. (d) Pipek, J.; Mezey, P. G. *J. Chem. Phys.* **1989**, *90*, 4916.

(18) Bickelhaupt, F. M.; Baerends, E. J. *Angew. Chem., Int. Ed.* **2003**, *42*, 4183.

(19) Mo, Y.; Wu, W.; Song, L.; Lin, M.; Zhang, Q.; Gao, J. *Angew. Chem., Int. Ed.* **2004**, *43*, 1986.

(20) Weinhold, F. *Angew. Chem., Int. Ed.* **2003**, *42*, 4188.
(21) Bohn, R. K. *J. Phys. Chem. A* **2004**, *108*, 6814.
(22) Schleyer, P. v. R.; Kaupp, M.; Hampel, F.; Bremer, M.; Mislowt, K. *J. Am. Chem. Soc.* **1992**, *114*, 6791.
(23) Wheland, G. W. *Resonance in Organic Chemistry*; Wiley: New York, 1955.
(24) (a) Li, X.; Zhang, Q. *Int. J. Quantum Chem.* **1989**, *36*, 599. (b) Zhang, Q.; Li, X. *J. Mol. Struct.* **1989**, *189*, 413.
(25) Mo, Y.; Lin, Z.; Wu, W.; Zhang, Q. *J. Phys. Chem.* **1996**, *100*, 11569.
(26) (a) Hoffman, R.; Shaik, S.; Hiberty, P. C. *Acc. Chem. Res.* **2003**, *36*, 750. (b) Shaik, S.; Hiberty, P. C. *Helv. Chim. Acta* **2003**, *86*, 1063.
(27) (a) Cooper, D. L., Ed. *Valence Bond Theory*; Elsevier: Amsterdam, 2002. (b) Mcweeny, R. *Int. J. Quantum Chem.* **1999**, *74*, 87. (c) Dijkstra, F.; van Lenthe, J. H. *J. Chem. Phys.* **2000**, *113*, 2100. (d) Thorsteinsson, T.; Cooper, D. L. *J. Math. Chem.* **1998**, *23*, 105.
(28) (a) Cooper, D. L.; Gerratt, J.; Raimondi, M. *Chem. Rev.* **1991**, *91*, 929. (b) Hiberty, P. C. *THEOCHEM* **1997**, *398*−*399*, 35.
(29) Wu, W.; Wu, A.; Mo, Y.; Lin, M.; Zhang, Q. *Int. J. Quantum Chem.* **1998**, *67*, 287.
(30) Wu, W.; Song, L.; Mo, Y.; Zhang, Q. *XMVB*−*An ab initio spin-free valence bond (VB) program*; Xiamen University: Xiamen, 2000.
(31) Coulson, C. A.; Fischer, I. *Philos. Mag.* **1949**, *40*, 386.
(32) Cooper, D. L.; Gerratt, J.; Raimondi, M. *Nature* **1986**, *323*, 699.
(33) (a) Gordon, M. S.; Neubauer, L. *J. Am. Chem. Soc.* **1974**, *96*, 5690. (b) Urban, J.; Schreiner, P. R.; Vacek, G.; Schleyer, P. v. R.; Huang, J. Q.; Leszczynski, J. *Chem. Phys. Lett.* **1997**, *263*, 441. (c) Halpern, A. M.; Glendening, E. D. *J. Chem. Phys.* **2003**, *119*, 11186.
(34) (a) Hay, P. J.; Wadt, W. R. *J. Chem. Phys.* **1985**, *82*, 270. (b) Hay, P. J.; Wadt, W. R. *J. Chem. Phys.* **1985**, *82*, 299.
(35) Check, C. E.; Faust, T. O.; Bailey, J. M.; Wright, B. J.; Gilbert, T. M.; Sunderlin, L. S. *J. Phys. Chem. A* **2001**, *105*, 8111.
(36) Frisch, M. J.; Trucks, G. W.; Schlegel, H. B.; Scuseria, G. E.; Robb, M. A.; Cheeseman, J. R.; Zakrzewski, V. G.; Montgomery, J. A. J.; Stratmann, R. E.; Burant, J. C.; Dapprich, S.; Millam, J. M.; Daniels, A. D.; Kudin, K. N.; Strain, M. C.; Farkas, O.; Tomasi, J.; Barone, V.; Cossi, M.; Cammi, R.; Mennucci, B.; Pomelli, C.; Adamo, C.; Clifford, S.; Ochterski, J.; Petersson, G. A.; Ayala, P. Y.; Cui, Q.; Morokuma, K.; Malick, D. K.; Rabuck, A. D.; Raghavachari, K.; Foresman, J. B.; Cioslowski, J.; Ortiz, J. V.; Baboul, A. G.; Stefanov, B. B.; Liu, G.; Liashenko, A.; Piskorz, P.; Komaromi, I.; Gomperts, R.; Martin, R. L.; Fox, D. J.; Keith, T.; Al-Laham, M. A.; Peng, C. Y.; Nanayakkara, A.; Challacombe, M.; Gill, P. M. W.; Johnson, B.; Chen, W.; Wong, M. W.; Andres, J. L.; Gonzalez, C.; Head-Gordon, M.; Replogle, E. S.; Pople, J. A.; Gaussian 98, revision A.9; Gaussian, Inc.: Pittsburgh, PA, 1998.
(37) Mo, Y.; Peyerimhoff, S. D. *J. Chem. Phys.* **1998**, *109*, 1687.
(38) Mo, Y. *J. Org. Chem.* **2004**, *69*, 5563.
(39) Kistiakowsky, G. B.; Ruhoff, J. R.; Smith, H. A.; Vaughan, W. E. *J. Am. Chem. Soc.* **1936**, *57*, 876.
(40) Durig, J. R.; Church, J. S. *J. Chem. Phys.* **1980**, *73*, 4784.
(41) Chattaraj, P. K.; Nath, S.; Sannigrahi, A. B. *J. Phys. Chem.* **1994**, *98*, 9143.